wxAMPS theoretical study of the bandgap structure of CZTS thin film to improve the device performance*

WANG Yanping (王延平), **WANG Jiao** (王姣), **LI Haoran** (李浩然), **ZHAO Aimei** (赵爱美), **LI Bing** (李冰), **BI Jinlian** (毕金莲)**, **and LI Wei** (李微)**

Tianjin Key Laboratory of Film Electronic and Communication Devices, School of Electrical and Electronic Engineering, Tianjin University of Technology, Tianjin 300384, China

(Received 19 October 2020; Revised 9 December 2020)

The carrier recombination was one of the factors limiting the further improvement of the Cu_2ZnSnS_4 (CZTS) thin film solar cells. In this paper, a proper bandgap structure was designed to solve this problem. The effects of the different bandgap structure on the CZTS thin film solar cells were studied by the solar cell performance simulation software wxAMPS. A graded bandgap structure was designed and optimized. The bandgap with a front bandgap gradient and a flat bandgap gradient had a favorable effect on the CZTS thin film solar cells. Finally, the fill factor (*FF*) and conversion efficiency (η) of the CZTS thin film solar cell were increased from 36.41% to 42.73% and from 6.85% to 10.03%, respectively. In addition, the effect of donor and acceptor defect densities in CZTS absorber layer near the CdS/CZTS interface on the device performance was studied, η of the CZTS thin film solar cell was increased from 5.99% to 7.55% when the acceptor defect concentration was 10^{12}—10^{13} cm^{-3}. Moreover, the thicknesses of the CZTS absorber layer were optimized. The *FF* and η of the CZTS thin film solar cell were increased to 63.41% and 15.04%, respectively.

Document code: A **Article ID:** 1673-1905(2021)08-0475-7

DOI https://doi.org/10.1007/s11801-021-0159-6

At present, solar cells already have mature production technology, thin film solar cells, such as cadmium telluride (CdTe), copper indium diselenide (CIS), copper indium gallium diselenide (CIGS) thin film solar cells, have been commercialized. However, the toxic Cd and expensive In/Ga contained in the ingredients greatly limit the further development of the CdTe, CIS, and CIGS thin film solar cells. Therefore, new alternative and environmentally friendly materials are needed, such as copper zinc tin sulphur Cu_2ZnSnS_4 (CZTS) and $Cu_2ZnSn(S_x, Se_{1-x})_4$ (CZTSSe) materials[1]. As a quaternary semiconductor compound, CZTS has a direct bandgap which can be adjusted between 1.4—1.57 eV, and the light absorption coefficient is greater than 10^4 cm^{-1}. The constituent elements (Cu, Zn, Sn, S) are non-toxic, low cost, and sufficient in the earth. At present, CZTS thin films can be prepared by various techniques, such as sputtering[2], evaporation[3], spray-pyrolysis[4], electrodeposition[5], and sol-gel method[6], etc. The sol-gel method with the advantages of green, non-toxic, low cost, and easy to realize industrialization is favored by researchers. Moreover, the CZTS thin film solar cell with the highest efficiency of 12.6% is prepared by the sol-gel method[6]. However, it is far behind the theoretical conversion efficiency of CZTS (32%) thin film solar cells[7] and the highest record conversion efficiency of CIS (23.35%) thin film solar cells[8]. The main factor restricting the further improvement of the CZTS thin film solar cells is carrier recombination, which leads a low minority carrier lifetime. This further causes the reduction of the open-circuit voltage (V_{oc}) and the short-circuit current density (J_{sc}) of CZTS thin film solar cells[9-11]. Therefore, the carrier recombination of the CZTS absorber layer must be solved to further improve the device performance.

Many studies have reported that the bandgap gradient could effectively reduce the carrier recombination. Mohammadnejad et al[12] showed a new bandgap gradient structure (including front and back bandgap gradient) of the CZTSSe absorber layer, and confirmed that the bandgap gradient structure affects carrier recombination. Ferhati et al[13] reported that the front bandgap gradient structure will introduce an extra electric field, which would lead to reduce the recombination losses. Amiri et al[14] presented a double layer with a 2.5 μm constant bandgap CZTS absorber layer being prepared on a 1.8 μm graded bandgap CZTSSe absorber layer. The study had shown that the efficiency was increased to 21.37% and the existence of the constant bandgap layer could reduce the probability of carrier recombination. In addition, studies have shown that defect passivation can more directly reduce carrier recombination. Arbouz et al[15] reported that the increase of defect density which will cause a stronger recombination of photo-generated carriers in the CZTS absorber layer. Mostefaoui et al[16]

* This work has been supported by the National Natural Science Foundation of China (No.61804108).

** E-mails: bijinlian815@126.com; cliwei618@126.com

showed a CIGS-based solar cell without defects state, and confirmed high defect density in p-CIGS layer lead to pronounced decrease in the photovoltaic parameters.

However, they did not study the influence of the bandgap structure on the lifetime of minority carriers (τ_n), and there is no research on the defect state in the CZTS absorber layer near the CZTS/CdS interface, for these we conducted a detailed study. In this paper, the influence of the position of the minimum bandgap point (the position of the front bandgap gradient structure) in the bandgap structure on the device performance was studied. Two different bandgap structure were designed: the first structure was a front bandgap gradient applied to the 2.0 μm CZTS absorber layer; the second structure was a flat bandgap layer introduced near the back of the CZTS absorber layer on the basis of the first structure. The influence of the bandgap structure on the minority carrier lifetime of CZTS absorber layer were studied, and the best bandgap gradient structure was determined to obtain the high conversion efficiency devices. Moreover, the effect of type and density of defects in the CZTS absorber layer near the CdS/CZTS interface on the device performance was studied, the optimal defect type and density with improved CZTS device performance was determined. Additionally, the effect of CZTS absorber layer thickness on the device performance was investigated, and the optimized CZTS absorber layer thickness with the highest conversion efficiency was obtained.

The software wxAMPS is a solar cell simulation software developed by the author in cooperation with Nankai University and the University of Illinois at Urbana-Champaign. There are three steps to simulate solar cells by wxAMPS: define the working environment of the device, such as temperature, spectrum, bias voltage, potential barrier at the electrode, and interface recombination rate, etc; enter the parameters of each layer; run the simulation to view the results.

The simulated performances of ZnO/CdS/CZTS thin film solar cell are shown in Fig.1. The thicknesses of ZnO layer, CdS layer and CZTS layer are 0.1 μm, 0.02 μm and 2.0 μm, respectively. The CZTS layer was subdivided into 100 layers with each layer thickness of 0.02 μm. The parameters of each layer are summarized and listed in Tab.1. Additionally, the thickness of CZTS absorber layer is optimized in this paper. The bandgap of CZTS material is adjustable in the range of 1.4—1.57 eV, which is very suitable for the solar spectrum. The direct band of CZTS increases from 1.32 eV to 1.69 eV with decreasing [Cu/(Zn+Sn)] and increases from 1.34 eV to 1.63 eV with increasing [Zn/Sn][17]. The compositional ratios of [Cu/(Zn+Sn)] and [Zn/Sn] were determined by the thickness of copper, tin and zinc sulphide films. Therefore, the bandgap gradients of CZTS absorbers can be changed by changing the compositions of CZTS layer. Tab.2 lists the bandgap gradient slopes of the CZTS thin films.

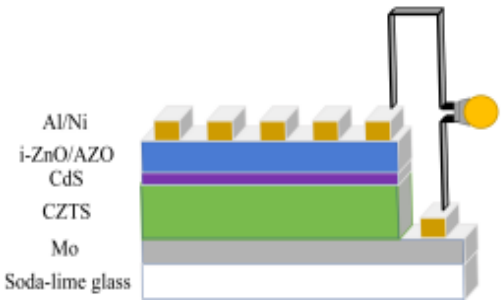

Fig.1 Structure diagram of the CZTS thin film solar cell

Tab.1 Parameters of each layer in the simulation of the ZnO/CdS/CZTS thin film solar cell

Quantity	Layer		
	n-ZnO	n-CdS	p-CZTS
ε_r	9	10	10
E_g (eV)	3.3	2.4	Variable
χ_e (eV)	4.3	4.2	4.4
N_c (cm^{-3})	2.2×10^{18}	1.8×10^{19}	2.2×10^{18}
N_v (cm^{-3})	1.8×10^{19}	2.2×10^{18}	1.8×10^{19}
μ_n (cm^2/V s)	100	100	100
μ_p (cm^2/V s)	25	25	25
Thickness (μm)	0.2	0.02	2.0

Tab.2 Bandgap gradient slopes of the CZTS thin films

Samples	Bandgap range (eV)	Slope (eV/μm)
A-1	1.40—1.40	0.000
A-2	1.41—1.40	0.005
A-3	1.45—1.40	0.025
A-4	1.49—1.40	0.045
A-5	1.53—1.40	0.065
A-6	1.57—1.40	0.085

The lattice mismatch at the CdS/CZTS interface induces lots of recombination centers existed at the CdS/CZTS interface. To reduce the CdS/CZTS interface recombination, a front gradient bandgap structure was introduced by increasing the surface bandgap. As shown in Fig.2, a front bandgap gradient of the CZTS absorber layer was designed. An additional electric field was introduced by increasing the surface bandgap of the CZTS absorption layer, which can further reduce the recombination probability of the minority carriers effectively and increase the lifetime of the carriers[17].

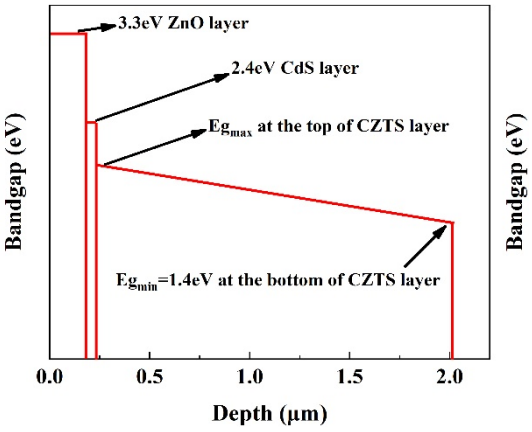

Fig.2 Structure of the front bandgap gradient of the CZTS absorber layer

Fig.3 shows the effects of the different slope of bandgap gradients on the saturation current density (J_o), open-circuit voltage (V_{oc}), J_{sc}, and conversion efficiency (η) of CZTS device, named as A-1, A-2, A-3, A-4, A-5, A-6 samples. In Fig.3(a), J_o of solar cell is one of the important parameters to evaluate device performance. J_o determines the maximum value of V_{oc}[18]. V_{oc}, J_{sc} and J_o can be described by the following equations[19]

$$V_{oc}=\left(\frac{kT}{q}\right)\ln\left(J_{sc}/J_o+1\right), \tag{1}$$

$$J_{sc}=q\overline{Q}\left(L_p+L_n\right), \tag{2}$$

$$J_o=q\left(\frac{D_n n_{po}}{L_n}+\frac{D_p p_{no}}{L_p}\right), \tag{3}$$

where T is room temperature, q is element charge, k is Boltzmann's constant, D_n/D_p is minority carrier diffusion coefficient in p-type/n-type, n_{po}/p_{no} is minority carrier concentration in p-type/n-type, L_n/L_p is minority carrier diffusion length in p-type/n-type, Q is the average generation rate of non-equilibrium carriers within the diffusion length (L_p+L_n) of the p-n junction. Since the two conditions in Eq.(3) are similar, if only for p-type semiconductors, combine Eqs.(4) and (5), Eq.(3) can be simplified as Eq.(6)[19]:

$$L_n=\sqrt{D_n\tau_n}\ , \tag{4}$$

$$p_{po}\cdot n_{po}=N_A\cdot n_{po}=n_i^2, \tag{5}$$

$$J_o\approx\frac{qD_n n_{po}}{L_n}=q\frac{n_i^2}{N_A}\sqrt{\frac{D_n}{\tau_n}}\ . \tag{6}$$

It can be seen from Eq.(1), V_{oc} increases with the reducing of the J_o. Moreover, refer to Eqs.(4), (5) and (6), q is element charge, D_n is minority carrier diffusion coefficient in p-type, L_n is minority carrier diffusion length in p-type, n_{po}/p_{po} is minority/majority carrier concentration in p-type, p_{po} and N_A are both majority carrier concentration in p-type, n_i is intrinsic carrier concentration. q, n_i, N_A and D_n are the constants determined by the properties of the material and will not change. Therefore, the determine factor of J_o is the lifetime of minority carrier (τ_n).

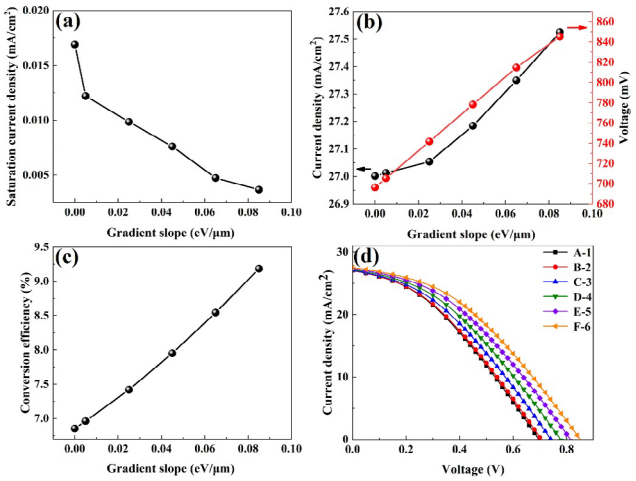

Fig.3 (a) Saturation current density, (b) V_{oc} and J_{sc}, (c) η, and (d) *J-V* curves of the CZTS thin film solar cells with different slopes of bandgap gradients

In Fig.3(a), J_o of the CZTS device decreases with the slope of the front bandgap gradient increases. It is because an additional electric field was introduced by the front bandgap gradient in the CZTS absorption layer, which can increase τ_n and decrease J_o. Besides, the maximum value of V_{oc} was determined by J_o (as shown in Fig.3(b)). The superior open-circuit voltage can be attributed to the decrease of J_o and the increase of minority carrier lifetime. The additional electric field provided by the front bandgap gradient, which promotes the movement of electrons from the P region to the p-n junction, reducing the probability of being recombined in the space charge region (SCR)[18]. Therefore, the existence of the additional electric field is equivalent to increase the photo-current and improve the short-circuit current density (as shown in Fig.3(b)). The improvement of the conversion efficiency of the front bandgap gradient can be attributed to the existence of the additional electric field, which more effectively reduces the probability of minority carriers being recombined and increases the lifetime of minority carriers. Finally, the conversion efficiency of CZTS solar cells increased to 9.18% with the slope of the front bandgap gradient of 0.085 (as shown in Fig.3(c)).

Tab.3 lists the details of CZTS devices performance with different front bandgap gradients. An additional electric field was introduced by the front bandgap gradient in the CZTS absorption layer, which promotes the movement of electrons in the P region to the p-n junction. This will reduce the probability of being recombined and increase the lifetime of minority carrier in the SCR. The higher slope of the front bandgap gradient will provide the stronger movement of electrons in the P region to the p-n junction in the SCR, which will increase open-circuit voltage, there will improve the conversion efficiency.

From the above, the additional electric field was introduced by a steep front gradient bandgap with the slope of 0.085, which improved the device performance (as shown in Fig.3(d)).

Tab.3 Device parameters of CZTS thin film solar cells with different front bandgap gradients

Samples	Slopes	V_{oc} (mV)	J_{sc} (mA/cm^2)	FF (%)	η (%)
A-1	0	696.4	27.00	36.41	6.85
A-2	0.005	705.4	27.01	36.52	6.96
A-3	0.025	741.8	27.05	36.96	7.41
A-4	0.045	778.3	27.18	37.57	7.95
A-5	0.065	814.8	27.34	38.33	8.54
A-6	0.085	844.0	27.52	39.19	9.18

Another bandgap structure with a flat bandgap layer (as shown in Fig.4(a)) located at the back of the CZTS absorber is simulated. The slope of the front bandgap gradient of CZTS absorber was set as 0.085, and the value of the flat bandgap is 1.4 eV, which will help to absorb more photons and convert into more electron-hole pairs. The width of the flat bandgap layer is set as x. Fig.4(b) shows the SCR of the CZTS thin film. The SCR of the CZTS is about 400 nm. Effects of x on the saturation current density, V_{oc}, J_{sc}, and η are shown in Fig.5. In Fig.5(a), it can be found that the saturation current density has a minimum value when x is 700 nm. According to Eq.(6), the minority carrier lifetime determines the saturation current density, it means that the minority carrier lifetime has a maximum value at 700 nm. Additionally, it can be seen from Eq.(2) that the determine factor of the short-circuit current density is the diffusion length of minority carriers (L_p+L_n), and the relationship between the diffusion length and the lifetime of minority carriers can be determined by Eqs.(4) and (7)[19]:

$$L_p = \sqrt{D_p \tau_p} \ . \tag{7}$$

Therefore, the short-circuit current density (as shown in Fig.5(b)) is inversely proportional to that of saturation current density, which has a maximum value with x of 700 nm. When x is greater than 700 nm, the minority carrier lifetime begins to decrease, meaning more carrier recombination centers are introduced into the back contact area to increase the minority carrier recombination rate.

As shown in Fig.5(b), we can find that the open-circuit voltage increases with the decrease of x. The increase in open-circuit voltage can be attributed to high separation of carriers. With x decreasing, the distance of the front bandgap is increase which will introduce an additional electric field in space charge region. There will have more carriers being separated, which will result into a high terminal voltage under open-circuit conditions. However, the width of the SCR of CZTS absorption layer is 400 nm (as shown in Fig.4(b)). When x is less than 1 500 nm, the minimum bandgap is outside the SCR, a reverse electric field was introduced outside the space electric field under thermal equilibrium condition, which will result the saturation of the open-circuit voltage. Therefore, the proper thickness of x can improve the CZTS device conversion efficiency (as shown in Fig.5(c)).

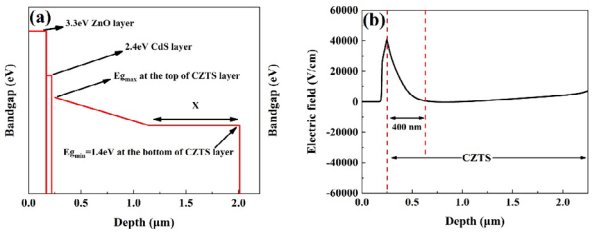

Fig.4 (a) Bandgap structure of the CZTS absorber layer (a flat bandgap layer with the thickness of x being added); (b) Space charge region of the CZTS thin film solar cells

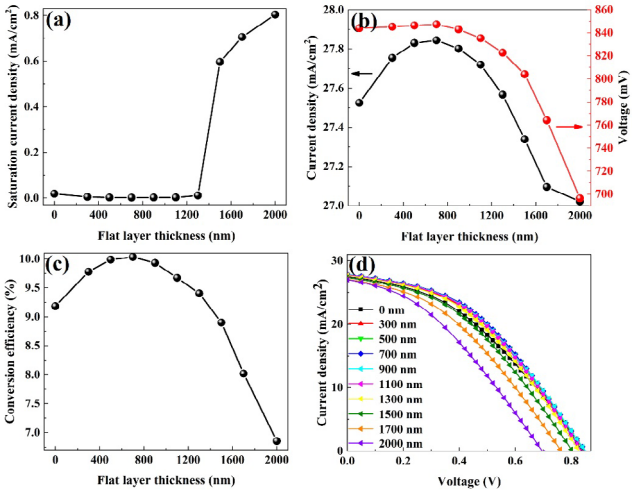

Fig.5 (a) Saturation current density, (b) V_{oc} and J_{sc}, (c) η, and (d) J-V curves of the CZTS thin film solar cells with different flat layer thicknesses x

The performances of CZTS devices with different flat bandgap layers are listed in Tab.4. When x is between 1 500—2 000 nm, the front bandgap gradient is in the space charge region. With the decrease of x, the recombination of the photo-generated carriers is reduced. The lifetime of photo-generated carriers at the back of the CZTS absorber layer is increased, which improve the CZTS device performances (as shown in Fig.5(d)). When x is less than 1 500 nm, the front bandgap gradient is outside the space charge region. With the decrease of x, there will introduce a reverse electric field outside the space electric field under thermal equilibrium conditions. This will result into an increase of the minority carrier

recombination rate. Finally, x of 700 nm is the most beneficial to improve the CZTS device performances (as shown in Fig.5(d)).

Tab.4 Device parameters of CZTS thin film solar cells with different flat layer thicknesses *x*

Samples	x (nm)	V_{oc} (mV)	J_{sc} (mA/cm^2)	FF (%)	η (%)
B-1	0	844.0	27.52	39.19	9.18
B-2	300	845.3	27.75	41.51	9.77
B-3	500	846.4	27.81	42.40	9.98
B-4	700	847.3	27.84	42.73	10.03
B-5	900	845.7	27.80	42.57	9.93
B-6	1 100	828.3	27.63	41.81	9.57
B-7	1 300	822.7	27.56	41.16	9.40
B-8	1 500	804.0	27.33	40.48	8.90
B-9	1 700	764.1	27.09	38.73	8.01
B-10	2 000	696.4	27.02	36.41	6.85

The optimized CZTS bandgap structure includes a steep front bandgap gradient with the slope of 0.085 and a flat bandgap layer with a thickness of 700 nm. Fig.6 shows the *J-V* curves of the CZTS devices before and after bandgap optimization. The bandgap of CZTS absorption layer is 1.4 eV with the thickness of 2.0 μm before optimization. In Fig.6, the optimized bandgap structure can more effectively reduce the probability of the minority carriers being recombined and increase the lifetime of carriers, which greatly improved the device performances.

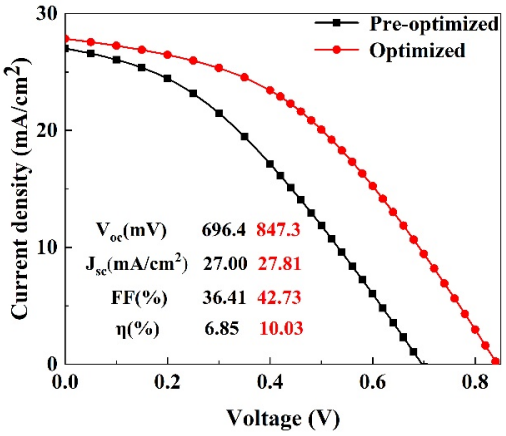

Fig.6 *J-V* curves of the CZTS thin film solar cells with the optimized bandgap structure

Optimized bandgap structure is indeed conducive to the improvement of device performance. However, defect passivation is an effective measure to improve the carrier collection and reduce the probability of carrier recombination[15,16]. We changed the density of different defects in the CZTS absorber layer near the CdS/CZTS interface (about 100 nm). The effect of defect type and density in the CZTS absorber layer near the CdS/CZTS interface on the device performance is studied.

As shown in Fig.7, acceptor defects have a greater impact on device performance than donor defects. As the acceptor defect density decreasing, it is favorable to improve the performance of the device, meaning more carrier recombination centers are introduced into the SCR region and the collection of carriers is reduced. According to whether the defect provides electrons or holes to the semiconductor, the types of defects were divided into donor defects and acceptor defects. The donor defect provides electrons to the semiconductor, so it is located at the bottom of the conduction band; The acceptor defect provides holes to the semiconductor, so it is on top of the valence band. In the CZTS absorption layer, the conductivity of CZTS was determined by holes as the majority carrier. In addition, the main defects of Cu_{Zn} and V_{Cu} in CZTS absorption layer are both acceptor defects, so the density of acceptor defects has a greater impact on the performance of CZTS devices.

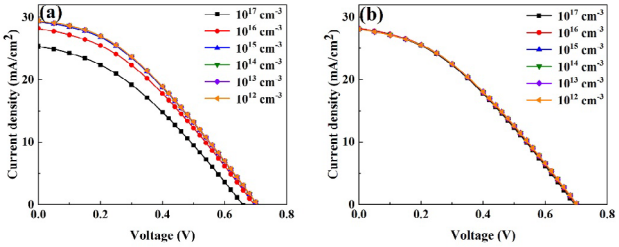

Fig.7 *J-V* curves of CZTS thin film solar cells with different densities of (a) acceptor defect and (b) donor defect

As shown in Tabs.5 and 6, the performance of the CZTS device remains unchanged, when the defect concentration is less than 10^{13} cm^{-3}. However, J_{sc} and V_{oc} show a downward trend when the defect density increases from 10^{13} cm^{-3} to 10^{17} cm^{-3}. This is induced by carrier recombination centers caused by defects, which are introduced into the SCR region. Additionally, the fill factor (FF) and η of the CZTS device are reduced, which is attributed to the increase in the probability of carrier recombination and the decrease in carrier lifetime. Passivating the defects in the CZTS absorption layer near the CdS/CZTS interface, which can reduce the probability of photo-generated carriers being recombined in the SCR region. When the defect concentration is 10^{13}—10^{12} cm^{-3}, the CZTS device has the best performance. In addition, the acceptor defect density has a greater impact on the performance of CZTS devices than the donor defect.

The influence of the absorber thickness on the CZTS device with the optimized bandgap structure is studied. The photon absorption and conversion ability of the

Tab.5 Device parameters of CZTS thin film solar cells with different densities of acceptor defect

Samples	V_{oc} (mV)	J_{sc} (mA/cm^2)	*FF* (%)	η (%)
10^{17} cm^{-3}	658.1	25.28	35.87	5.99
10^{16} cm^{-3}	694.7	28.20	36.25	7.10
10^{15} cm^{-3}	704.9	29.25	36.36	7.49
10^{14} cm^{-3}	706.1	29.40	36.38	7.54
10^{13} cm^{-3}	706.2	29.41	36.39	7.55
10^{12} cm^{-3}	706.2	29.42	36.39	7.55

absorption layer is important for CZTS absorber layer. The thickness of the absorber has a great influence on the absorption and conversion ability of photons. As shown in Fig.8(a), the *EQE* increases with the decrease of the absorber thickness in the visible wavelength range of 400—700 nm, meaning the carrier collection in thin CZTS film is better than that in thick CZTS film. It is because the photo-generated carriers diffuse longer before being collected in thick CZTS absorbers, which results into the increase of the recombination rate[20]. However, the absorption of the incident photons was decreasing with the thickness of CZTS absorber decrease. The increased recombination and the inadequate light absorption will both deteriorate the device performance of CZTS solar cells. That is why J_{sc} and η don't increase continuously with the increase of the CZTS thickness (as shown in Fig.8(b)).

Tab.6 Device parameters of CZTS thin film solar cells with different densities of donor defect

Samples	V_{oc} (mV)	J_{sc} (mA/cm^2)	*FF* (%)	η (%)
10^{17} cm^{-3}	694.7	28.05	36.25	7.10
10^{16} cm^{-3}	700.1	28.12	36.34	7.18
10^{15} cm^{-3}	702.5	28.16	36.54	7.20
10^{14} cm^{-3}	702.8	28.20	36.57	7.21
10^{13} cm^{-3}	702.8	28.21	36.57	7.21
10^{12} cm^{-3}	702.8	28.21	36.57	7.21

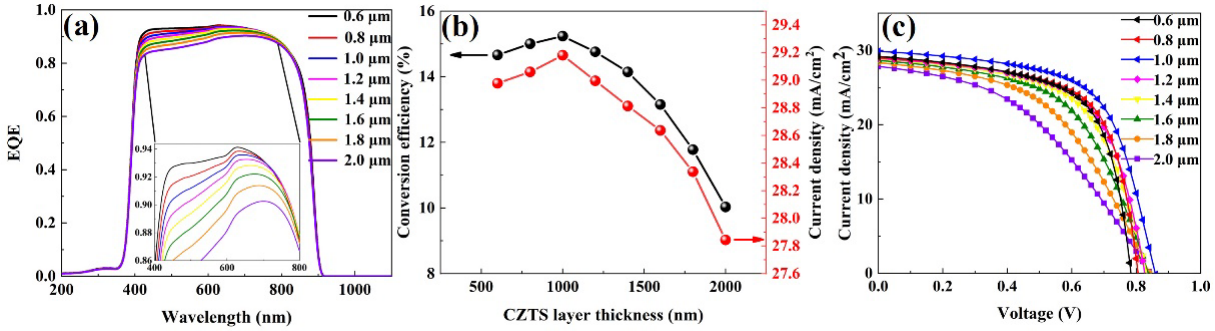

Fig.8 (a) *EQE*, (b) J_{sc} and η, and (c) *J-V* curves of CZTS thin film solar cells with different thicknesses of CZTS absorber layer

Tab.7 lists the device parameters of CZTS solar cells with different thicknesses of CZTS absorbers. As listed in Tab.7, when thicknesses of CZTS absorber layer is between 1.0—2.0 μm, the conversion efficiency of CZTS solar cells increases with the decreasing of the CZTS thickness. It may because that the diffusion length and the recombination probability of photo-generated carriers is reduced with the decreasing of the CZTS thickness, which improved the device performances. When the thickness is reduced to 1.0 μm, the conversion efficiency of CZTS solar cell is 15.04%. With the thickness below 1.0 μm, the conversion efficiency decreases. It is because the absorption of the incident photons reduced with thin CZTS absorber. The *FF* loss was caused by the changes in shunt resistance (R_{sh}) and series resistance (R_s). Higher R_{sh} and lower R_s can get *FF*. Tab.8 lists the R_{sh} and R_s of CZTS solar cells with different CZTS thicknesses. As listed in Tab.8, the 1.0-μm-thick CZTS absorber layer is with high R_{sh} and low R_s. Therefore, the optimal thickness of the CZTS absorber layer is 1.0 μm and the conversion efficiency is 15.04% (as shown in Fig.8(c)).

Tab.7 Detailed device parameters of CZTS solar cells with different CZTS thicknesses

Samples	V_{oc} (mV)	J_{sc} (mA/cm^2)	*FF* (%)	η (%)
2.0 μm-CZTS	847.3	27.84	42.73	10.03
1.8 μm-CZTS	848.1	28.33	49.40	11.77
1.6 μm-CZTS	849.0	28.63	54.85	13.15
1.4 μm-CZTS	849.7	28.81	58.96	14.14
1.2 μm-CZTS	850.6	28.91	61.73	14.75
1.0 μm-CZTS	851.4	29.18	63.41	15.04
0.8 μm-CZTS	850.8	29.03	62.17	15.00
0.6 μm-CZTS	850.1	28.97	61.17	14.66

In this paper, we studied the effect of the bandgap structure on the device performances of the CZTS solar cells with wxAMPS simulation software. It is confirmed that the steep front bandgap gradient with the slope of 0.085 combined with a 700 nm flat bandgap layer could well reduce the recombination and increase the life time of the photo-generated carriers. The corresponding *FF*

Tab.8 Shunt resistance and series resistance of CZTS solar cells with different CZTS thicknesses

Samples	R_{sh} ($\Omega \cdot cm^2$)	R_s ($\Omega \cdot cm^2$)
2.0 μm-CZTS	180.3	10.62
1.8 μm-CZTS	231.1	7.05
1.6 μm-CZTS	272.7	5.55
1.4 μm-CZTS	304.1	2.71
1.2 μm-CZTS	322.6	1.40
1.0 μm-CZTS	327.4	0.17
0.8 μm-CZTS	317.2	0.53
0.6 μm-CZTS	293.7	5.98

and η of CZTS solar cell are increased from 36.41% to 42.73% and from 6.85% to 10.03%, respectively. Moreover, the effect of defect type and density in the CZTS absorber layer near the CdS/CZTS interface on the device performance was investigated. The acceptor defect density had a greater impact on the performance of CZTS devices than the donor defect density. The η of the CZTS thin film solar cell was increased from 5.99% to 7.55% when the acceptor defect concentration was 10^{12}—10^{13} cm^{-3}. Additionally, the thickness of the CZTS absorber layer was optimized with the thickness of 1.0 μm. Finally, the highest simulation η of CZTS thin film solar cell is 15.04%.

References

[1] Aydin R and Akyuz I, Optik **200**, 163407 (2020).

[2] Fernandes P A, Salomé P M P and Cunha A F, Thin Solid Films **517**, 2519 (2019).

[3] Naoufel K, Chamekh S and Kanzari M, Sol. Energy **207**, 496 (2020).

[4] Babichuk I S, Semenmenko M O and Caballero R, Sol. Energy **205**, 154 (2020).

[5] Xu J T, Yang J and Jiang S X, Ceram. Int. **46**, 25927 (2020).

[6] Wang W, Winkler M T, Gunawan O, Gokmen T, Todorov T K, Zhu Y and Mitzi D B, Adv. Energy Mater. **4**, 1301465 (2014).

[7] Wang J, Yu N and Zhang Y, J. Alloys Compd. **688**, 923 (2016).

[8] Yoshida S, Solar Frontier Achieves World Record Thin-Film Solar Cell Efficiency of 23.35%, Int. Conf. Prop. Steam, 2 (2019).

[9] Cherouana A and Labbani R, Appl. Surf. Sci. **424**, 251 (2017).

[10] Tchognia J H N, Arba Y, Dakhsi K, Hartiti B, Ridah A, Ndjaka J M and Thevenin P, Optimization of the Output Parameters in Kesterite-Based Solar Cells by AMPS-1D, In Proceedings of the 3rd International Renewable and Sustainable Energy Conference (IRSEC), 1 (2015).

[11] Maykel C, Valencia-Resendiz E, Pulgarín-Agudelo F A and Vigil-Galán O, Solid-State Electron. **118**, 1 (2016).

[12] Mohammadnejad S and Parashkouh A B, Appl. Phys. A: Mater. Sci. Process. **123**, 758 (2017).

[13] Ferhati H and Djeffal F, Opt. Mater. **76**, 393 (2018).

[14] Amiri S, Dehghani S and Safaiee R, Opt. Quantum Electron. **52**, 323 (2020).

[15] Arbouz H, Aissat A and Vilpot J P, Int. J. Hydrogen Energy. **42**, 8827 (2017).

[16] Mostefaoui M, Mazari H and Khelifi S, Energy Procedia. **74**, 736 (2015).

[17] Adewoyin A D, Olopade M A and Chendo M, Opt. Quantum Electron. **49**, 336 (2017).

[18] Jinqun S, Haiyan Q, Zhiyao M and Xuemei Z A, J. Huazhong Univ. Sci. Technol. **29**, 24 (2016). (in Chinese)

[19] Neamen D A, The Physics of Semiconductors, 7th ed, Enke L, Jinsheng L, Publishing House of Electronics Industry: Beijing, China, 155 (2011).

[20] Cetinkaya S, Optik **181**, 627 (2019).